Early prediction of the efficacy of local epicardial radiofrequency ablation for the robotic treatment of persistent atrial fibrillation

Daniele Salvi, MS,[1] Eduardo Celentano, MD, FHRS,[2] Ernesto Cristiano, MD,[2] Stefano Schena, MD,[3] Alfonso Agnino, MD,[4] Ettore Lanzarone, MS, PhD[1]

From the [1]Department of Management, Information and Production Engineering, University of Bergamo, Dalmine (BG), Italy, [2]Department of Electrophysiology, Humanitas Gavazzeni Hospital, Bergamo, Italy, [3]Division of Cardiothoracic Surgery, Medical College of Wisconsin, Milwaukee, Wisconsin, and [4]Division of Robotic and Minimally Invasive Cardiac Surgery, Humanitas Gavazzeni Hospital, Bergamo, Italy.

BACKGROUND Early prediction of the efficacy of local epicardial radiofrequency ablation (LERFA) is crucial for optimizing the robotic treatment of persistent atrial fibrillation.

OBJECTIVE This study aimed to develop a machine learning model that accurately predicts LERFA efficacy within the first 5 seconds of the procedure, to stop ineffective procedures and reduce unnecessary cardiac tissue damage.

METHODS Impedance data from 92 patients who underwent robotic LERFA were analyzed, with a total of 2486 LERFAs included in the final dataset. LERFA efficacy predictors, including zero-time impedance value, slope, and harmonic components, were extracted from the first 5 seconds of each time-impedance curve. Several supervised machine learning approaches were then tested to predict LERFA efficacy.

RESULTS Random Forest demonstrated the highest performance, achieving 94.5% accuracy, 88.3% sensibility, and 97.2% specificity. This Random Forest model significantly outperformed the benchmark approach based on the zero-time impedance value alone, which achieved an accuracy of only 55.6% and a specificity of only 37.7%.

CONCLUSION The developed model enables fast and accurate prediction of LERFA efficacy, potentially reducing the number of completed LERFAs by 56.8%. This reduction results in minimal damage to cardiac tissue, a lower risk of complications, a reduction in operating time, and greater precision and safety in the ablation process.

KEYWORDS Persistent atrial fibrillation; Local epicardial radiofrequency ablation; Robotic treatment; Early discontinuation; Machine learning

(Heart Rhythm O^2 2026;7:2–8)

Introduction

Atrial fibrillation (AF) is among the most prevalent cardiac arrhythmias, affecting millions of patients each year worldwide. Among the various forms of AF, persistent AF, and long-standing persistent AF present significant clinical challenges.[1–4] These subtypes are often resistant to conventional treatments, including pharmacological therapy, cardioversion, and catheter ablation, and associated with a higher risk of severe complications, such as stroke and heart failure. Traditional endocardial catheter ablation has limited efficacy, with a success rate of around 55% in persistent AF, as shown in the CAPLA trial.[2] In contrast, hybrid treatment strategies combining local epicardial radiofrequency ablation (LERFA) and endocardial ablation achieved efficacy rates >75% in observational studies.[5,6]

This improvement was attributed to the addition of epicardial ablation lines, which target both endocardial and epicardial tissues to achieve transmural ablation.[2] Furthermore, the introduction of robotic technology has facilitated enhanced surgical precision, more accurate movements within the chest, improved device positioning, and greater stability during energy delivery, leading to better clinical outcomes.[5]

However, despite higher success rates, the remaining ineffective LERFAs result in unnecessary damage to the cardiac tissue, which can lead to severe complications, including epicardial bleeding, atrioesophageal fistula, phrenic nerve damage, and death. The main factors contributing to an ineffective LERFA include: (1) incorrect positioning of the ablator device; (2) presence of abundant

Address reprint requests and correspondence: Dr Ettore Lanzarone, Department of Management, Information and Production Engineering, University of Bergamo, Via A. Einstein 2, 24044 Dalmine (BG), Italy. E-mail address: ettore.lanzarone@unibg.it.

2666-5018/

https://doi.org/10.1016/j.hroo.2025.10.003

KEY FINDINGS

- A timely prediction of the efficacy of local epicardial radiofrequency ablation (LERFA) is provided, to stop ineffective LERFAs within 5 seconds.
- In our procedure, LERFA efficacy parameters are extracted from the first 5 seconds of time-impedance curves, and a Machine Learning model predicts LERFA efficacy based on them.
- Several ML models are compared to find out the best one.
- Among the tested models, Random Forest achieved 94.5% accuracy, 88.3% sensibility, and 97.2% specificity.
- Our results show that the proposed approach enables a reduction in the number of completed LERFAs by 56.8% with respect to the benchmark approach.

adipose tissue and atrial fibrosis; (3) involuntary movement of the device during the ablation; and (4) proximity to the left atrial appendage, which generates a signal that interferes with ablation.

Electrical impedance plays a crucial role in assessing LERFA efficacy. Research has shown that a decrease in impedance by at least 10 Ω is required to achieve effective local tissue ablations[7,8] for both endocardial and epicardial treatments.[6,9,10]

Successful LERFAs are generally characterized by a steady and continuous decrease in impedance over time, whereas unsuccessful LERFAs often lack this consistent decrease. For instance, proximity to the left atrial appendage often results in a U-shaped pattern. Examples of effective and ineffective LERFA time-impedance curves are reported in Figure 1.

In this context, it is essential to develop an online system capable of predicting LERFA efficacy in the shortest possible time, that is, in the first few seconds, and to promptly discontinue the procedure in the event of an ineffective LERFA. However, in Figure 1, it can be clearly seen that the differences in time-impedance curves are not so evident in the first few seconds, making it difficult to anticipate the future time course of the impedance signal and thus LERFA efficacy.

Current clinical practice relies on the zero-time impedance value recorded at the beginning of the energy supply as a predictor of LERFA efficacy. Specifically, when this value exceeds the 120 Ω threshold, the likelihood of achieving an effective LERFA is greatly reduced, due to decreases in the contact force between the tissue and the device and in the electrical current.[11–13] In addition, a recent study attempted to identify a restricted number of biophysical parameters that correlate well with LERFA efficacy and can therefore predict LERFA outcome.[6]

This study aimed to develop a machine learning (ML) tool that accurately predicts LERFA efficacy from the first 5 seconds of the time-impedance curve, to be used in clinical practice as a useful tool to promptly discontinue ineffective procedures. This would increase the number of completed

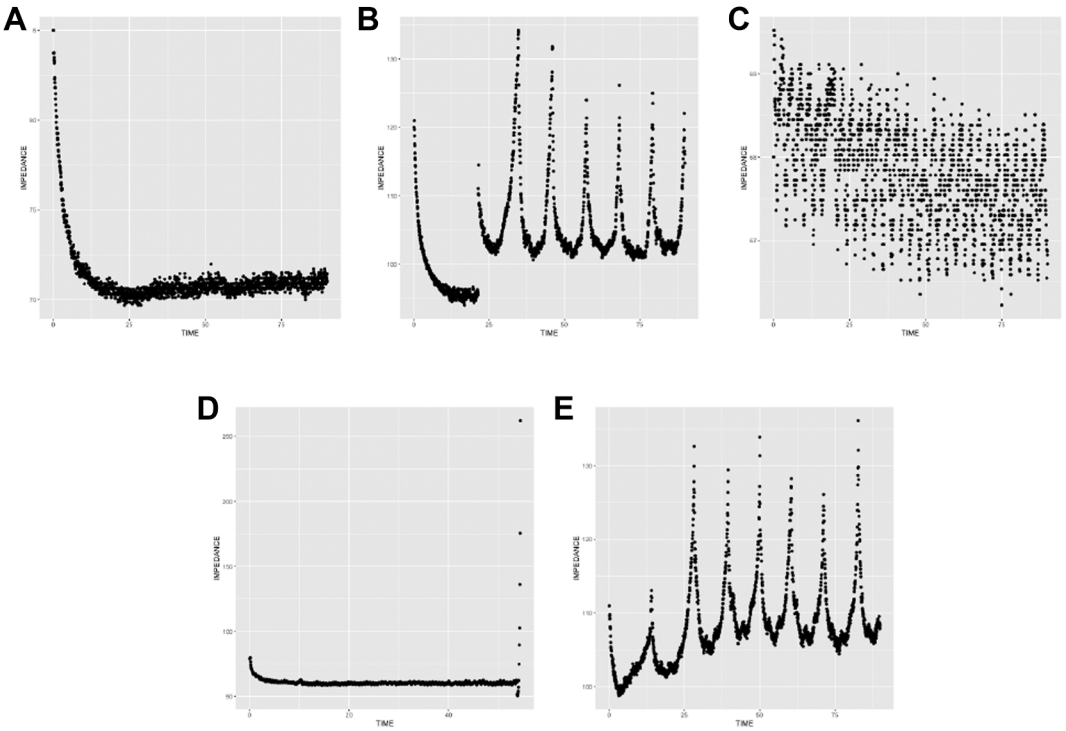

Figure 1 Examples of effective (**A**) and ineffective (**B–E**) LERFA time-impedance curves. LERFA = local epicardial radiofrequency ablation.

LERFA procedures that prove successful and reduce the risks associated with unnecessary injuries. Unlike Celentano et al,[6] we do not rely solely on the zero-time impedance value and a restricted set of parameters assessed a posteriori over the entire LERFA procedure. Instead, we exploit the full richness of the time-impedance signal, stopping at the first 5 seconds to allow predictive use of our tool in the clinic during LERFA procedures.

To validate our tool, we retrospectively applied it to patients undergoing robotic LERFA with the EPi-Sense ablator (AtriCure Inc, Mason, OH). Then, we used the standard practice based on the zero-time impedance value as a benchmark for comparison.

Methods

Enrolled population and data

We retrospectively analyzed a cohort of consecutive patients who underwent hybrid LERFA of persistent AF or long-standing persistent AF performed with the EPi-Sense ablator and robotic surgery between 2020 and 2023 at the Heart and Vascular Center, Center for Advanced Care, Froedtert Hospital/Medical College of Wisconsin, Milwaukee, WI.

The research adhered to the Declaration of Helsinki. The authors were in compliance with the regulations of the respective institutional review boards on human studies and animal care and use committees, and obtained patient consent where appropriate.

The procedure was performed in all patients as previously described,[14] according to the 2020 European Society of Cardiology guidelines.[15] All patients were operated on by the same surgeon. The treated patients, aged 18–75 years, met at least 2 of the following criteria:

- No response or intolerance to at least 2 classes of anti-arrhythmic drugs;
- Previously failed percutaneous AF ablation procedures;
- Evident risk factors for AF recurrences after transcatheter ablation, including body mass index >30 kg/m^2, left atrial volume index >40 mL/m^2, and AF duration >24 months.

We then applied the following exclusion criteria to the potential participants: prior surgical ablation; acute myocardial infarction; any surgical intervention within the past 3 months; left atrial thrombus identified via pre-procedural imaging; left ventricular ejection fraction $<40\%$; a thromboembolic event (eg, transient ischemic attack, ischemic stroke, or pulmonary embolism) within the past 12 months; New York Heart Association functional class IV; and unfeasible single-lung ventilation. These criteria resulted in a sample of 92 patients with a total of 2576 LERFAs.

Data from each energy delivery were recorded and digitized using the EPi-Sense system at a sampling frequency of 20 Hz, corresponding to 1 sample every 0.05 seconds. They were collected for 90 seconds from the start of each ablation cycle. The dataset included the following variables:

- Time-impedance curve;
- Power delivered by the device over time;
- Current supplied by the device over time;
- Voltage applied between the electrode and the cardiac tissue over time, used to stabilize power delivery in response to impedance fluctuations.

The target power, defined as the preset power level that the device aims to maintain throughout the procedure, was known for each delivery.

Each delivery was retrospectively classified as either 0 (ineffective LERFA) or 1 (effective LERFA) by a team of expert electrophysiologists from the Froedtert Hospital/Medical College (Milwaukee, WI, USA) and the Humanitas Gavazzeni Hospital (Bergamo, Italy). Effective LERFA is defined as the completion of a single RFA with disappearance of the atrial electrogram after the application of the radiofrequency energy, that is, with a post-ablation electrogram with bipolar voltage <0.05 mV.

Only the first 5 seconds of each time-impedance curve, corresponding to 100 data points, were used, as the objective was to classify LERFA in the first 5 seconds. Therefore, deliveries manually interrupted before 5 seconds were excluded from the analysis. Following this exclusion criterion, the final dataset was reduced to 2486 LERFAs. Among them, 1734 (69.8%) were classified as unsuccessful (ineffective 0), and 752 (30.2%) as effective (classification 1).

LERFA impedance parameters and predictors

A total of 33 numerical parameters were extracted from the first 5 seconds of each time-impedance curve. They were based on the time-impedance curve itself, its slope calculated as the difference between impedance values at successive discrete time points, and its harmonic components extracted with the Fourier transform. They are listed below:

- Zero-time impedance – parameter IMP_0;
- Impedance values at 1, 2, 3, 4, and 5 seconds;
- Maximum and minimum impedance values;
- Impedance drops over time intervals [0,1], [0,2], [0,3], [0,4], and [0,5] seconds;
- First 3 values of impedance slope – parameters $SLOPE_1$, $SLOPE_2$, and $SLOPE_3$;
- Mean and variance of the impedance slope over the 5 seconds – parameters $MEAN_{SL}$ and VAR_{SL};
- Amplitudes of the first 6 harmonic components – parameters $AMPL_1$ (constant component), $AMPL_2$, $AMPL_3$, $AMPL_4$, $AMPL_5$, and $AMPL_6$;
- Mean and variance of the above amplitudes;
- Phases of the first 6 harmonic components – parameters $PHASE_2$, $PHASE_3$, $PHASE_4$, $PHASE_5$, and $PHASE_6$ (phase of the first component is always equal to 0 and therefore not included);
- Mean and variance of the above phases.

The spectral analysis for obtaining amplitudes and phases was carried out by calculating the Fourier transform of the time-impedance signal using the Cooley-Tukey algorithm.[16] We observed that a fair reconstruction of the signal can be obtained with 6 harmonic components. This is why the

amplitudes and the phases of only the first 6 harmonic components were included.

We conducted a first analysis to assess the parameter correlations and identify the most relevant predictors for the classification task. Highly correlated parameters were excluded from the predictors to reduce redundancy, and the selection of parameters to be retained within correlated groups was guided by consultations with experienced electrophysiologists.

ML models

A very simple and well explainable ML model was considered at first to provide a baseline for comparing other more complex approaches. It consisted of a logistic regression, in which a selection of predictors was included using the Akaike's information criterion.[17] Predicted probabilities were then binarized with a classification threshold determined as the average of the mean predicted probabilities for the 2 groups (ineffective with observed classification 0, and effective with observed classification 1) within the training and validation sets.

Afterward, following a strategy already exploited in the literature,[18–20] several supervised ML models were tested and compared, and the one that minimized the classification error was selected. More specifically, the following approaches were considered:

- 5 penalized regressions based on the Elastic Net Regularization, with coefficient a set to 0 (Ridge regression), 0.25, 0.5, 0.75, and 1 (Lasso regression);
- Random forest (RF), which combines several decision trees to generate the final prediction[21];
- Bayesian additive regression trees;
- Support vector machine with either linear, polynomial, or radial kernels;
- Adaptive splines.

For those with a continuous output, binarization was performed with a threshold of 0.5.

All of these were implemented in R.[22] Details on the employed R packages are provided in Table 1.

A K-fold cross-validation approach was employed to validate all ML models, with $K = 5$ folds containing approximately the same number of ablations. To avoid overfitting, each fold was designed in such a way as to ensure that all the data of a given patient were entirely contained in one fold. The same $K = 5$ folds were kept for all ML models. Then, depending on the specific ML model, a further subdivision into training and validation sets of the K-1 folds used to train the model was carried out at each K-fold iteration. In each iteration, of the ablations used to the train the ML model, approximately 80% constituted the training set and 20% the validation set. This proportion was kept unchanged across methods, with the exception of Elastic Net Regularization, which does not require a validation set for interval validation. The percentage of effective lesions in the 5 folds was: 33.2% in fold 1; 25.4% in fold 2; 28.7% in fold 3; 35.6% in fold 4; 28.0% in fold 5. These values gave, in the training set of the different repetitions, percentages close to that of the entire population (30.2%).

Table 1 R packages employed to implement the considered ML models

Model	R package
Logistic regression	stats
AIC	mass
ENR	glmnet
RF	randomForest
BART	bartMachine
SVM	e1071
Adaptive splines	earth

AIC = Akaike's information criterion; BART = Bayesian additive regression trees; ENR = Elastic Net Regularization; ML = machine learning; RF = Random Forest; SVM = support vector machine.

Results

Selected predictors

The correlation coefficients are detailed in the Supplemental Table 1. On the basis of these correlation coefficients, a visual representation of the correlations by means of scatterplots and consultations with experienced electrophysiologists, the following 17 parameters were included as predictors for the ML models: IMP_0, $SLOPE_1$, $SLOPE_2$, $SLOPE_3$, $MEAN_{SL}$, VAR_{SL}, $AMPL_1$, $AMPL_2$, $AMPL_3$, $AMPL_4$, $AMPL_5$, $AMPL_6$, $PHASE_2$, $PHASE_3$, $PHASE_4$, $PHASE_5$, and $PHASE_6$.

Logistic regression

The Akaike's information criterion selected 11 variables from the 17 predictors: IMP_0, $SLOPE_1$, $MEAN_{SL}$, VAR_{SL}, $AMPL_1$, $AMPL_3$, $AMPL_6$, $PHASE_2$, $PHASE_3$, $PHASE_5$, and $PHASE_6$. Estimated model coefficients for these predictors (and the intercept) are reported in Table 2.

Table 2 Estimated coefficients with significance levels for the logistic regression with AIC

Predictor	Model coefficient	Significance
Intercept	-1.532	***
IMP_0	-0.325	****
$SLOPE_1$	-0.100	****
$MEAN_{SL}$	-23.83	****
VAR_{SL}	-0.059	*
$AMPL_1$	0.0032	****
$AMPL_3$	-0.0039	
$AMPL_6$	-0.0210	****
$PHASE_2$	-0.708	****
$PHASE_3$	-0.775	****
$PHASE_5$	-0.239	
$PHASE_6$	-0.167	

Significance codes: ****$P < 0.001$; ***$P < 0.01$; **$P < 0.05$; * $P < 0.01$; empty for not significant.

AIC = Akaike's information criterion.

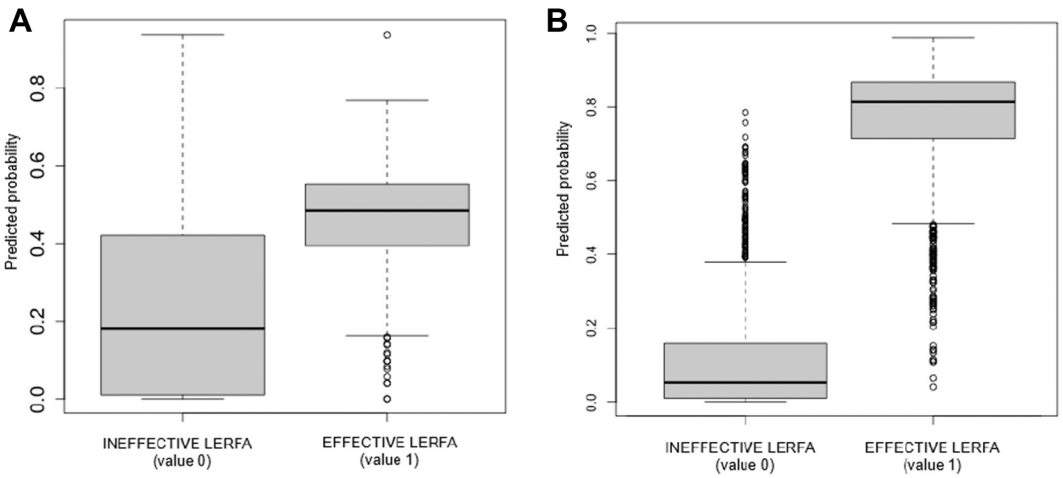

Figure 2 Boxplots of the predicted probabilities for the 2 groups (observed classification 0 vs 1), obtained from the logistic regression with AIC (**A**) and RF (**B**). AIC = Akaike's information criterion; LERFA = local epicardial radiofrequency ablation; RF = Random Forest.

A boxplot of the predicted probabilities in cross-validation for the 2 groups (ineffective LERFA with observed classification 0 and effective LERFA with observed classification 1) is shown in Figure 2A. The 2 distributions of predicted probabilities were significantly different (*P*-value of the 2-sided Wilcoxon rank-sum test <0.001) despite the presence of some outliers.

The predicted probabilities were finally binarized as described in Section 2.3, with a resulting threshold of 0.35. The corresponding confusion matrix under cross-validation is reported in Table 3A, which corresponds to an accuracy of 71.7%, a sensibility of 82.4%, and a specificity of 67.1%.

This fully explainable model, in which the impact of each predictor can be easily assessed via its coefficient, showed limited predictive capabilities. This is why we also considered other more complex ML models.

Other ML models

The results from the analyzed ML models are reported in Table 4 in terms of accuracy, sensibility, and specificity under cross-validation.

The results showed the highest performance for RF, which achieved an accuracy of 94.5%, a sensibility of 88.3%, and a specificity of 97.2%. In our opinion, this is linked to the greater flexibility of RF compared with the other models, which allowed it to capture the relationships between data and the variability of observations.

The corresponding confusion matrix, reported in Table 3B, confirms very low and similar values outside the principal diagonal. They refer to an optimized number of decision trees set to 600, determined to achieve an effective trade-off between accuracy and computational time for training.

We now look at the RF results in detail. The boxplots in Figure 2B demonstrate that the predicted probabilities are significantly different for the 2 groups even if some outliers are present (ineffective LERFA with observed classification 0, and effective LERFA with observed classification 1), as further confirmed by a *P*-value < 0.001 on the 2-sided Wilcoxon rank-sum test.

Finally, it is worth mentioning that computational time for inference of the developed RF is less than 1 second.

Table 3 Confusion matrix under cross-validation for the logistic regression with AIC (A) and RF (B)

(A)

		Predicted outcome	
		Ineffective (0)	Effective (1)
True outcome	Ineffective (0)	1163	571
	Effective (1)	132	620

(B)

		Predicted outcome	
		Ineffective (0)	Effective (1)
True outcome	Ineffective (0)	1686	48
	Effective (1)	88	664

AIC = Akaike's information criterion; RF = Random Forest.

Table 4 Accuracy, sensibility, and specificity from the tested ML models under cross-validation

		Accuracy (%)	Sensibility (%)	Specificity (%)
ENR	Ridge	68.1	21.9	88.1
	a = 0.25	70.2	36.7	84.8
	a = 0.5	70.4	37.6	84.6
	a = 0.75	70.3	38.2	84.3
	Lasso	70.1	36.8	84.6
RF		94.5	88.3	97.2
BART		75.9	58.9	83.0
SVM	linear	68.6	8.1	95.6
	polynomial	69.6	0.0	99.7
	radial	73.2	56.4	80.8
Adaptive splines		75.3	55.9	83.7

BART = Bayesian additive regression trees; ENR = Elastic Net Regularization; ML = machine learning; RF = Random Forest; SVM = support vector machine.

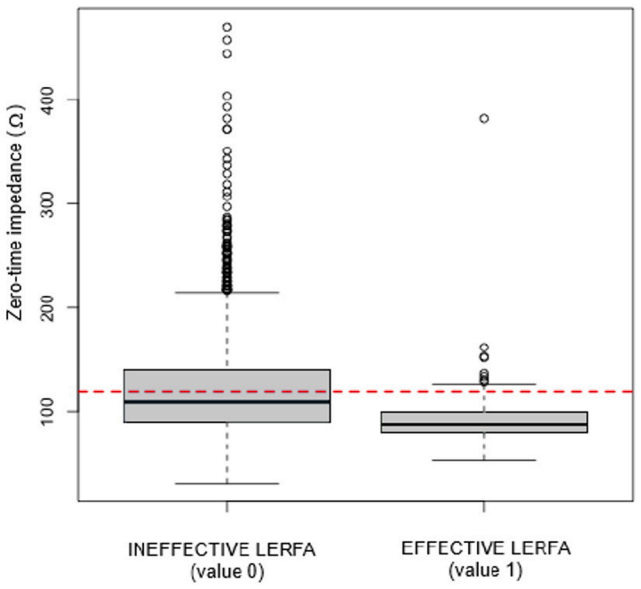

Figure 3 Boxplots of the zero-time impedance for the 2 groups (observed classification 0 vs 1). The *red dashed line* indicates the threshold impedance of 120 Ω. LERFA = local epicardial radiofrequency ablation.

Comparison with benchmark approach

The zero-time impedance alone, which is the standard practice currently adopted, was used as a benchmark for comparison and applied to our dataset.

The boxplots of the zero-time impedance stratified by LERFA classification are presented in Figure 3. They reveal that the effective LERFAs (classified as 1) almost never exhibit an initial impedance value exceeding the 120 Ω threshold. However, it is possible to obtain an ineffective LERFA (classified as 0) even when the initial impedance value is below the threshold.

A more detailed analysis was then conducted by constructing the contingency matrix in Table 5, which illustrates the binary classification based on the 120 Ω threshold.

This contingency matrix, based on the zero-time impedance value alone, shows that LERFA efficacy can be predicted with a low accuracy of only 55.6%, a low specificity of only 37.7%, and a good sensibility of 96.9%. Therefore, all the methods proposed herein improve predictions compared with setting currently adopted in clinical practice.

Table 5 Contingency matrix between classification (IMP_0 over threshold) and class

		Zero-time impedance	
		>120 Ω (bad)	<120 Ω (good)
True outcome	Ineffective (0)	654	1,080
	Effective (1)	23	729

Discussions and conclusion

In this work, we challenged several ML models with the task of accurately predicting LERFA efficacy from the first 5 seconds of the time-impedance curve. The goal was to provide a useful tool for clinical practice that promptly supports discontinuation of ineffective LERFAs.

Unlike previous research in the literature and current clinical practice, we do not rely solely on the zero-time impedance value nor evaluate parameters a posteriori over the entire LERFA procedure after its completion. On the contrary, we exploit only the first 5 seconds of the time-impedance signal to allow predictive use of our tool during the first few instants of LERFA procedures.

All ML models we proposed outperformed conventional clinical practice, which is characterized by low accuracies. Among them, RF offered highly accurate predictions of LERFA efficacy, which corresponded to completing 1.07 LERFAs with predicted efficacy to actually obtain an effective one. With the current clinical practice relying only on the zero-time impedance, this number increased up to 2.48, demonstrating that RF can reduce the number of completed LERFAs by 56.8%. This reduction translates into multiple clinical benefits, including minimized cardiac tissue damage, a lower risk of procedure-related complications, reduced operative time, and decreased risk associated with temperature elevations. Additionally, this reduction shortens the overall procedure time, enhancing both the precision and safety of the ablation process.

The proposed RF is also fast enough to meet the goal of predicting LERFA efficacy during treatment, with a computational time for inference of less than 1 second. In this way, predicting LERFA efficacy takes less than 6 seconds, that is, 5 seconds to collect the first part of the time-impedance curve plus the computational time for RF inference and other negligible software times.

Limitations and future extensions

Only variation in the impedance signal was analyzed in this study. However, other variables may be of interest for further analysis, even if not directly related to the impedance signal, and could be included in future studies. These variables include personal information, stage of the disease, medications taken, position of ablation on the heart, and morphological features of the heart, such as hypertrophy. Exploring the role of these additional features could help to assess whether, in addition to the impedance signal, other factors can be predictive of the response to treatment or the course of the pathology.

Furthermore, we considered ablation discontinuation without evaluating lesion duration, which may be another important outcome to evaluate in the future.

Finally, the same approach could be extended to other treatments, for example, endocardial ablation during hybrid procedures, once sufficient data has been collected from these treatments.

Funding Sources: This paper has been published with the financial support of Cliniche Gavazzeni SpA.

Disclosures: The authors have no conflicts of interest to disclose.

Authorship: All authors attest they meet the current ICMJE criteria for authorship.

Patient Consent: The authors obtained patient consent where appropriate.

Ethics Statement: The research adhered to the Helsinki Declaration. The authors were in compliance with the regulations of the respective institutional review boards on human studies and animal care and use committees.

Appendix

Supplementary data

Supplementary data associated with this article can be found in the online version at https://doi.org/10.1016/j.hroo.2025.10.003

References

1. Griffin M, Calvert P, Gupta D. Persistent atrial fibrillation ablation: ongoing challenges defining the target population and substrate. Curr Treat Options Cardiovasc Med 2023;25:461–475.
2. Kistler PM, Chieng D, Sugumar H, et al. Effect of catheter ablation using pulmonary vein isolation with vs without posterior left atrial wall isolation on atrial arrhythmia recurrence in patients with persistent atrial fibrillation: the CAPLA randomized clinical trial. JAMA 2023;329:127–135.
3. Roka A, Burright I. Remodeling in persistent atrial fibrillation: pathophysiology and therapeutic targets — a systematic review. Physiologia 2023;3:43–72.
4. Sharp AJ, Pope MT, Briosa E, Gala A, Varini R, Banerjee A, Betts TR. Identifying extra pulmonary vein targets for persistent atrial fibrillation ablation: bridging advanced and conventional mapping techniques. Europace 2025;27:euaf048.
5. Agnino A, Giroletti L, Graniero A, et al. Robotic-assisted epicardial hybrid ablation and left appendage closure in persistent atrial fibrillation: first European experience. J Clin Med 2024;13:1563.
6. Celentano E, Cristiano E, Schena S, et al. Local epicardial robotic-enhanced hybrid ablation efficacy predictors for persistent atrial fibrillation. Heart Rhythm O2 2025;6:280–289.
7. Szegedi N, Perge P, Sallo Z, et al. The role of local impedance drop in the acute lesion efficacy during pulmonary vein isolation performed with a new contact force sensing catheter. Europace 2022;24(suppl 1):euac053–euac220.
8. Taylor M, Thornley A, Bates M, James S. Do radiofrequency ablation lesions titrated to impedance drop correlate with recommended empirical target parameters for catheter ablation of atrial fibrillation? Europace 2018;20(suppl 4):iv34–iv35.
9. Lepillier A, Maggio R, De Sanctis V, et al. Insight into contact force local impedance technology for predicting effective pulmonary vein isolation. Front Cardiovasc Med 2023;10:1169037.
10. Segreti L, De Simone A, Schillaci V, et al. A novel local impedance algorithm to guide effective pulmonary vein isolation in atrial fibrillation patients: preliminary experience across different ablation sites from the CHARISMA pilot study. J Cardiovasc Electrophysiol 2020;31:2319–2327.
11. Chinitz JS, Michaud GF, Stephenson K. Impedance-guided radiofrequency ablation: using impedance to improve ablation outcomes. J Innov Card Rhythm Manag 2017;8:2868–2873.
12. Oh S, Choe WS, Lee SR, Choi EK. Impedance drop determines ablation lesion volume at the same level of ablation index. Int J Arrhythm 2023;24:10.
13. Sanchez Somonte P, Martinez Cossiani M, Guido L, et al. Correlation between Lesions Size Index (LSI) and impedance dynamics during radiofrequency ablation for atrial fibrillation: impact of lesion duration and contact force. EP Europace 2024;26(suppl 1):euae102–euae200.
14. Schena S, Lindemann J, Carlson A, et al. Robotic-enhanced hybrid ablation for persistent and long-standing atrial fibrillation: early assessment of feasibility, safety, and efficacy. JTCVS Tech 2024;25:81–93.
15. Hindricks G, Potpara T, Dagres N, et al. 2020 ESC Guidelines for the diagnosis and management of atrial fibrillation developed in collaboration with the European Association for Cardio-Thoracic Surgery (EACTS): the Task Force for the diagnosis and management of atrial fibrillation of the European Society of Cardiology (ESC) Developed with the special contribution of the European Heart Rhythm Association (EHRA) of the ESC. Eur Heart J 2021;42:373–498.
16. Cooley JW, Tukey JW. An algorithm for the machine calculation of complex Fourier series. Math Comput 1965;19:297–301.
17. Bozdogan H. Model selection and Akaike's information criterion (AIC): the general theory and its analytical extensions. Psychometrika 1987;52:345–370.
18. Doneda M, Borsa VM, Brugnera A, et al. The predictive effects of resting-state and task-related prefrontal and vagal activity on cognitive performances. J Psychophysiol 2024;38:28–42.
19. Doneda M, Poloni S, Bozzetto M, Remuzzi A, Lanzarone E. Surgical planning of arteriovenous fistulae in routine clinical practice: a machine learning predictive tool. J Vasc Access 2024;25:1170–1179.
20. Webb CA, Cohen ZD, Beard C, Forgeard M, Peckham AD, Björgvinsson T. Personalized prognostic prediction of treatment outcome for depressed patients in a naturalistic psychiatric hospital setting: a comparison of machine learning approaches. J Consult Clin Psychol 2020;88:25.
21. Schonlau M, Zou RY. The random forest algorithm for statistical learning. STATA J 2020;20:3–29.
22. R Foundation for Statistical Computing. R: a language and environment for statistical computing. 2021. https://www.R-project.org. Accessed October 1, 2025.